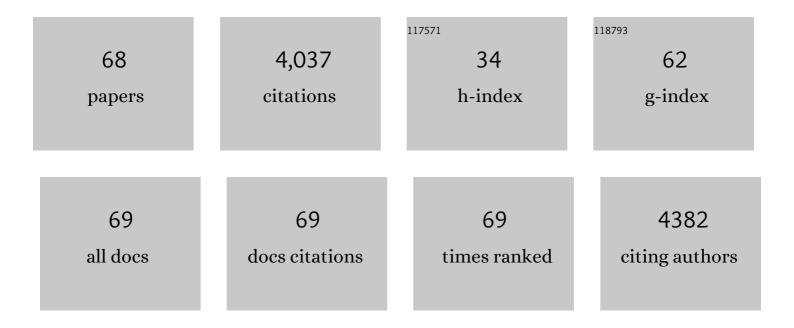
## Hui Chen

List of Publications by Year in descending order

Source: https://exaly.com/author-pdf/1011315/publications.pdf Version: 2024-02-01



HULCHEN

#	Article	IF	CITATIONS
1	Carbon-Armored Co <sub>9</sub> S <sub>8</sub> Nanoparticles as All-pH Efficient and Durable H <sub>2</sub> -Evolving Electrocatalysts. ACS Applied Materials & Interfaces, 2015, 7, 980-988.	4.0	335
2	Active Site Engineering in Porous Electrocatalysts. Advanced Materials, 2020, 32, e2002435.	11.1	304
3	Metallic Co <sub>9</sub> S <sub>8</sub> nanosheets grown on carbon cloth as efficient binder-free electrocatalysts for the hydrogen evolution reaction in neutral media. Journal of Materials Chemistry A, 2016, 4, 6860-6867.	5.2	265
4	Activating Inert, Nonprecious Perovskites with Iridium Dopants for Efficient Oxygen Evolution Reaction under Acidic Conditions. Angewandte Chemie - International Edition, 2019, 58, 7631-7635.	7.2	176
5	High-performance oxygen evolution electrocatalysis by boronized metal sheets with self-functionalized surfaces. Energy and Environmental Science, 2019, 12, 684-692.	15.6	169
6	Transitionâ€Metal–Boron Intermetallics with Strong Interatomic d–sp Orbital Hybridization for Highâ€Performance Electrocatalysis. Angewandte Chemie - International Edition, 2020, 59, 3961-3965.	7.2	139
7	Promoting Subordinate, Efficient Ruthenium Sites with Interstitial Silicon for Ptâ€Like Electrocatalytic Activity. Angewandte Chemie - International Edition, 2019, 58, 11409-11413.	7.2	128
8	Activating Inert, Nonprecious Perovskites with Iridium Dopants for Efficient Oxygen Evolution Reaction under Acidic Conditions. Angewandte Chemie, 2019, 131, 7713-7717.	1.6	123
9	Revealing Activity Trends of Metal Diborides Toward pHâ€Universal Hydrogen Evolution Electrocatalysts with Ptâ€Like Activity. Advanced Energy Materials, 2019, 9, 1803369.	10.2	111
10	Ultrathin In <sub>2</sub> O <sub>3</sub> Nanosheets with Uniform Mesopores for Highly Sensitive Nitric Oxide Detection. ACS Applied Materials & Interfaces, 2017, 9, 16335-16342.	4.0	108
11	Perovskiteâ€īype Solid Solution Nanoâ€Electrocatalysts Enable Simultaneously Enhanced Activity and Stability for Oxygen Evolution. Advanced Materials, 2020, 32, e2001430.	11.1	107
12	Design of a Multilayered Oxygenâ€Evolution Electrode with High Catalytic Activity and Corrosion Resistance for Saline Water Splitting. Advanced Functional Materials, 2021, 31, 2101820.	7.8	103
13	Growth of molybdenum carbide micro-islands on carbon cloth toward binder-free cathodes for efficient hydrogen evolution reaction. Journal of Materials Chemistry A, 2015, 3, 16320-16326.	5.2	100
14	Porous Ga–In Bimetallic Oxide Nanofibers with Controllable Structures for Ultrasensitive and Selective Detection of Formaldehyde. ACS Applied Materials & Interfaces, 2017, 9, 4692-4700.	4.0	95
15	Intermetallic borides: structures, synthesis and applications in electrocatalysis. Inorganic Chemistry Frontiers, 2020, 7, 2248-2264.	3.0	94
16	Promoting Subordinate, Efficient Ruthenium Sites with Interstitial Silicon for Pt‣ike Electrocatalytic Activity. Angewandte Chemie, 2019, 131, 11531-11535.	1.6	92
17	A high surface area flower-like Ni–Fe layered double hydroxide for electrocatalytic water oxidation reaction. Dalton Transactions, 2015, 44, 11592-11600.	1.6	90
18	Transitionâ€Metal–Boron Intermetallics with Strong Interatomic d–sp Orbital Hybridization for Highâ€Performance Electrocatalysis. Angewandte Chemie, 2020, 132, 3989-3993.	1.6	88

Ниі Снем

#	Article	IF	CITATIONS
19	Optimization of Active Sites via Crystal Phase, Composition, and Morphology for Efficient Lowâ€Iridium Oxygen Evolution Catalysts. Angewandte Chemie - International Edition, 2020, 59, 19654-19658.	7.2	79
20	Revealing the Relationship between Energy Level and Gas Sensing Performance in Heteroatom-Doped Semiconducting Nanostructures. ACS Applied Materials & Interfaces, 2018, 10, 29795-29804.	4.0	74
21	Electrospinning Synthesis of Bimetallic Nickel–Iron Oxide/Carbon Composite Nanofibers for Efficient Water Oxidation Electrocatalysis. ChemCatChem, 2016, 8, 992-1000.	1.8	69
22	<i>In situ</i> structural evolution of a nickel boride catalyst: synergistic geometric and electronic optimization for the oxygen evolution reaction. Journal of Materials Chemistry A, 2019, 7, 5288-5294.	5.2	69
23	lridium-containing water-oxidation catalysts in acidic electrolyte. Chinese Journal of Catalysis, 2021, 42, 1054-1077.	6.9	66
24	Well-Tuned Surface Oxygen Chemistry of Cation Off-Stoichiometric Spinel Oxides for Highly Selective and Sensitive Formaldehyde Detection. Chemistry of Materials, 2018, 30, 2018-2027.	3.2	64
25	A class of metal diboride electrocatalysts synthesized by a molten salt-assisted reaction for the hydrogen evolution reaction. Chemical Communications, 2019, 55, 8627-8630.	2.2	57
26	Enhanced sensing performance to toluene and xylene by constructing NiGa2O4-NiO heterostructures. Sensors and Actuators B: Chemical, 2019, 282, 331-338.	4.0	51
27	Enhanced Iridium Mass Activity of 6H-Phase, Ir-Based Perovskite with Nonprecious Incorporation for Acidic Oxygen Evolution Electrocatalysis. ACS Applied Materials & Interfaces, 2019, 11, 42006-42013.	4.0	48
28	Electrospinning preparation of mesoporous spinel gallate (MGa2O4; M Ni, Cu, Co) nanofibers and their M(II) ions-dependent gas sensing properties. Sensors and Actuators B: Chemical, 2017, 240, 689-696.	4.0	46
29	Crystal phase-dependent electrocatalytic hydrogen evolution performance of ruthenium–boron intermetallics. Chemical Communications, 2020, 56, 3061-3064.	2.2	44
30	Oxygen vacancy-rich, Ru-doped In <sub>2</sub> O <sub>3</sub> ultrathin nanosheets for efficient detection of xylene at low temperature. Journal of Materials Chemistry C, 2018, 6, 4156-4162.	2.7	42
31	Unique Electronic Structure in a Porous Gaâ€In Bimetallic Oxide Nanoâ€Photocatalyst with Atomically Thin Pore Walls. Angewandte Chemie - International Edition, 2016, 55, 11442-11446.	7.2	40
32	Graphene-nanosheet-wrapped LiV3O8 nanocomposites as high performance cathode materials for rechargeable lithium-ion batteries. Journal of Power Sources, 2016, 307, 426-434.	4.0	38
33	High-performance formaldehyde sensing realized by alkaline-earth metals doped In2O3 nanotubes with optimized surface properties. Sensors and Actuators B: Chemical, 2020, 304, 127241.	4.0	38
34	d–sp orbital hybridization: a strategy for activity improvement of transition metal catalysts. Chemical Communications, 2022, 58, 7730-7740.	2.2	37
35	Protonated Iridate Nanosheets with a Highly Active and Stable Layered Perovskite Framework for Acidic Oxygen Evolution. ACS Catalysis, 2022, 12, 8658-8666.	5.5	34
36	Alkali metal-incorporated spinel oxide nanofibers enable high performance detection of formaldehyde at ppb level. Journal of Hazardous Materials, 2020, 400, 123301.	6.5	33

Ниі Снем

#	Article	IF	CITATIONS
37	Multiple crystal phases of intermetallic tungsten borides and phase-dependent electrocatalytic property for hydrogen evolution. Chemical Communications, 2020, 56, 13983-13986.	2.2	32
38	Surface-clean, phase-pure multi-metallic carbides for efficient electrocatalytic hydrogen evolution reaction. Inorganic Chemistry Frontiers, 2019, 6, 940-947.	3.0	29
39	Identifying Key Structural Subunits and Their Synergism in Low-Iridium Triple Perovskites for Oxygen Evolution in Acidic Media. Chemistry of Materials, 2020, 32, 3904-3910.	3.2	29
40	Synthesis of porous In <sub>2</sub> O <sub>3</sub> microspheres as a sensitive material for early warning of hydrocarbon explosions. RSC Advances, 2015, 5, 5424-5431.	1.7	28
41	Light alloying element-regulated noble metal catalysts for energy-related applications. Chinese Journal of Catalysis, 2022, 43, 611-635.	6.9	27
42	Tailoring energy level and surface basicity of metal oxide semiconductors by rare-earth incorporation for high-performance formaldehyde detection. Inorganic Chemistry Frontiers, 2019, 6, 1767-1774.	3.0	25
43	Realization of interstitial boron ordering and optimal near-surface electronic structure in Pd-B alloy electrocatalysts. Chemical Engineering Journal, 2021, 419, 129568.	6.6	23
44	Interfacial engineering of ZIF-67 derived CoSe/Co(OH)2 catalysts for efficient overall water splitting. Composites Part B: Engineering, 2022, 236, 109823.	5.9	22
45	Precursor-mediated synthesis of double-shelled V <sub>2</sub> O <sub>5</sub> hollow nanospheres as cathode material for lithium-ion batteries. CrystEngComm, 2016, 18, 4068-4073.	1.3	21
46	Effects of impact energy on the wear resistance and work hardening mechanism of medium manganese austenitic steel. Friction, 2017, 5, 447-454.	3.4	20
47	Accelerated room-temperature crystallization of ultrahigh-surface-area porous anatase titania by storing photogenerated electrons. Chemical Communications, 2017, 53, 1619-1621.	2.2	19
48	Low-iridium electrocatalysts for acidic oxygen evolution. Dalton Transactions, 2020, 49, 15568-15573.	1.6	19
49	Non-catalytic, instant iridium (Ir) leaching: A non-negligible aspect in identifying Ir-based perovskite oxygen-evolving electrocatalysts. Chinese Journal of Catalysis, 2022, 43, 885-893.	6.9	17
50	Room temperature, fast fabrication of square meter-sized oxygen evolution electrode toward industrial alkaline electrolyzer. Applied Catalysis B: Environmental, 2022, 316, 121605.	10.8	17
51	Theoretical insights into nonprecious oxygen-evolution active sites in Ti–Ir-Based perovskite solid solution electrocatalysts. Journal of Materials Chemistry A, 2020, 8, 218-223.	5.2	15
52	Asymmetrically strained hcp rhodium sublattice stabilized by 1D covalent boron chains as an efficient electrocatalyst. Chemical Communications, 2021, 57, 5075-5078.	2.2	14
53	Crystal phase engineering of electrocatalysts for energy conversions. Nano Research, 2022, 15, 10194-10217.	5.8	13
54	Screening and Understanding Lattice Siliconâ€Controlled Catalytically Active Site Motifs from a Library of Transition Metalâ€Silicon Intermetallics. Small, 2022, 18, e2107371.	5.2	12

Ниі Снем

#	Article	IF	CITATIONS
55	Optimization of Active Sites via Crystal Phase, Composition, and Morphology for Efficient Lowâ€ŀridium Oxygen Evolution Catalysts. Angewandte Chemie, 2020, 132, 19822-19826.	1.6	11
56	Metal-Coordinating Single-Boron Sites Confined in Antiperovskite Borides for N <sub>2</sub> -to-NH <sub>3</sub> Catalytic Conversion. ACS Catalysis, 2022, 12, 2967-2978.	5.5	11
57	Enhanced electrochemical performance of Li3V2(PO4)3 microspheres assembled with nanoparticles embedded in a carbon matrix. RSC Advances, 2015, 5, 31410-31414.	1.7	9
58	Pt-decorated foam-like Ga-In bimetal oxide nanofibers for trace acetone detection in exhaled breath. Journal of Alloys and Compounds, 2021, 873, 159813.	2.8	9
59	Electronic and morphological dual modulation of NiO by indium-doping for highly improved xylene sensing. New Journal of Chemistry, 2022, 46, 3831-3837.	1.4	8
60	Surface-oxidized titanium diboride as cocatalyst on hematite photoanode for solar water splitting. CrystEngComm, 2022, 24, 2251-2257.	1.3	8
61	Enhanced formaldehyde sensing properties of IrO2-loaded porous foam-like Ga1.4In0.6O3 nanofibers with ultrathin pore walls. Journal of Alloys and Compounds, 2018, 732, 856-862.	2.8	6
62	Enhanced Electrochemical Activity and Chromium Tolerance of the Nucleation-Agent-Free La2Ni0.9Fe0.1O4+δCathode by Gd0.1Ce0.9O1.95 Incorporation. Electronic Materials Letters, 2018, 14, 432-439.	1.0	6
63	Olivine-type cadmium germanate: a new sensing semiconductor for the detection of formaldehyde at the ppb level. Inorganic Chemistry Frontiers, 2021, 8, 4467-4473.	3.0	6
64	Energy level regulation to optimize hydrogen sensing performance of porous bimetallic gallium-indium oxide with ultrathin pore walls. Sensors and Actuators B: Chemical, 2022, 350, 130864.	4.0	6
65	Crystal phase-selective synthesis of intermetallic palladium borides and phase-regulated (electro)catalytic properties. Catalysis Science and Technology, 0, , .	2.1	6
66	Unique Electronic Structure in a Porous Gaâ€In Bimetallic Oxide Nanoâ€Photocatalyst with Atomically Thin Pore Walls. Angewandte Chemie, 2016, 128, 11614-11618.	1.6	5
67	Future directions of catalytic chemistry. Pure and Applied Chemistry, 2021, 93, 1411-1421.	0.9	4
68	NumericalÂstudyÂonÂcharge transport and electrochemical performance of Gd and Pr co-doped ceria-based solid oxide fuel cells free from internal shorting. Ionics, 2022, 28, 3445-3452.	1.2	4